Asymmetric lattice Boltzmann model for shallow water flows

B. Chopard, P Van Thang, Laurent Lefevre

HAL Id: hal-01624987

https://hal.archives-ouvertes.fr/hal-01624987

Submitted on 27 Oct 2017

Asymmetric Lattice Boltzmann model for shallow water flows

B. Chopard[a], P. van Thang[b], L. Lefèvre[c,*]

[a]*University of Geneva, Switzerland*
[b]*GIPSA-Lab, Univ. Grenoble Alpes, F-38402 Saint-Martin d'Hères, France*
[c]*LCIS, Univ. Grenoble Alpes, F-26902 Valence, France*

Abstract

We consider a Galilean transformation of the lattice Boltzmann model for shallow water flows. In this new reference frame, the velocity lattice is asymmetrical but it is possible to simulate flows with Froude number larger than 1 and to model the transition from a torrential to a fluvial regime.

Keywords: shallow water equation, lattice Boltzmann, fluvial-torrential transition, Galilean transformation

1. Introduction

The shallow water (SW) equation describes a free surface flow with the approximation that the vertical component of the velocity flow is negligible with respect to the horizontal components. This description is adequate for systems having a wide spatial extent in the x- and y-axes but a small depth. The one-dimensional SW equations are often used to describe the flow in a canal. They read [1]

$$\partial_t h + \partial_x(hu) = 0$$

---

*Corresponding author, 50 rue Barthélémy de Laffémas, F-26902 Valence cedex 9, France Tel. +33.(0)4.75.75.94.64 ; Fax +33.(0)4.75.43.56.42
    Email addresses: Bastien.Chopard@unige.ch (B. Chopard),
Van-Thang.Pham@gipsa-lab.grenoble-inp.fr (P. van Thang),
Laurent.Lefevre@lcis.grenoble-inp.fr (L. Lefèvre)

$$\partial_t(hu) + \partial_x \left(\frac{1}{2}gh^2 + hu^2 \right) = F \tag{1}$$

where $h(x,t)$ is the height of the water column at location x along the canal length and at time t, and $u(x,t)$ is the velocity of that water column. The quantity g is the gravity constant. The force term $F = gh(I - J)$ accounts for the bed slope I and the bed friction J, where $I = \partial h_b/\partial x$ with h_b the bed height and J is modeled with the classical Manning formula [1]:

$$J = \frac{n^2 u^2}{\left(\frac{Bh}{B+2h} \right)^{4/3}} \tag{2}$$

with n the Manning coefficient and B the width of the canal.

The lattice Boltzmann (LB) approach to shallow water (SW) flows has been discussed by several authors [2, 3, 4]. One-dimensional applications are studied by Frandsen [5] and we recently proposed a very detailed analysis of the 1D model [6, 7] in the context of irrigation canals. In this study, we showed that the LB scheme is numerically faster than other standard methods, for the same accuracy. The LB SW approach is therefore a very interesting candidate to simulate a complex irrigation system, in view of its optimal management.

The Froude number Fr, defined as

$$\mathrm{Fr} = \frac{u_0}{\sqrt{gh_0}} \tag{3}$$

is an important dimensionless quantity to characterize flows in rivers. Here u_0 is the characteristic speed of the flow and h_0 the characteristic height of the water. The quantity $\sqrt{gh_0}$ being the speed of the surface waves, a Froude number smaller than 1 corresponds to a fluid that flows slower than the surface waves. This situation is termed the *fluvial regime*. On the other hand, when Fr is larger than 1, one has the so-called *torrential* regime, in which the fluid flows faster than the surface waves. Both regimes may be present in an irrigation

canal and the transition between them is important.

However, our previous study [6] shows that the LB SW model is numerically unstable for Froude numbers equal to or larger than 1. More precisely, we found that for a given height h_0, the numerical scheme requires a speed u_0 smaller than $\sqrt{gh_0}$. This prevents the LB model to reach the torrential regime.

In this paper, we consider the possibility to increase u_0 by defining a model in which the equilibrium state is not a rest fluid but a fluid with a constant flow $U > 0$. We show here that such a goal can be achieved by performing a Galilean transformation of the the initial 1D LB SW model.

The paper is organized as follows: a short summary of the one-dimensional LB SW model is given in section 2. Then, in section 3 we derived the new LB model, which will be based on an asymmetrical velocity lattice. In section 4 we validate our approach, in particular by simulating the transition from a torrential regime (Fr > 1) to a fluvial regime (Fr < 1). Finally, some conclusions are given in section 5.

2. The one-dimensional LB model

In the LB approach, the height $h(x,t)$ of a water column is split in several quantities $f_i(x,t)$. The value of f_i describes the part of the water column that travels with velocity v_i. Therefore the water level $h(x,t)$ and the velocity $u(x,t)$ of a fluid column are expressed in terms of distribution functions $f_i(x,t)$ as

$$h = \sum_i f_i, \quad hu = \sum_i v_i f_i \tag{4}$$

The standard one-dimensional LB SW model is defined on the so-called D1Q3 lattice (1 dimension and 3 velocities) and reads

$$f_i(x + v_i \Delta t, t + \Delta t) = f_i(x,t) + \frac{1}{\tau}(f_i^{eq} - f_i) \tag{5}$$

where i runs from 0 to 2 and the lattice velocities are defined in fig. 1. The

3

expression for the local equilibrium distributions is (see for instance [5, 6, 7])

$$
\begin{aligned}
f_0^{eq} &= h - \frac{1}{2v^2}gh^2 - \frac{1}{v^2}hu^2 \\
f_1^{eq} &= \frac{1}{4v^2}gh^2 + \frac{1}{2v}hu + \frac{1}{2v^2}hu^2 \\
f_2^{eq} &= \frac{1}{4v^2}gh^2 - \frac{1}{2v}hu + \frac{1}{2v^2}hu^2
\end{aligned}
\tag{6}
$$

where $v = \Delta x/\Delta t$, Δx is the lattice spacing and Δt the time step.

It can be shown [6, 7] that this model reproduces the shallow water equations (1) for $F = 0$. It is also shown that the stability region of the 1D-LB model is restricted to Fr ≤ 1 and the Courant's conditions

$$
-u + \sqrt{gh} < v \qquad -u - \sqrt{gh} > -v
\tag{7}
$$

These last equations indicate that the speed of the flow plus the speed of the wave must be smaller than the maximum speed v resolved by the model. Note that it is found [6] that the value of the relaxation time τ is not affecting the stability provided that $\tau > 1/2$.

3. The asymmetric LB model

3.1. The model

We now consider a Galilean transformation of the model of section 2. Under such a transformation, the lattice velocities are changed to $V_i = v_i + U$ where U is the speed of the new reference frame. In order to simulated a flow around Fr $= 1$, we choose $U = v/2$.

The D1Q3 lattice of fig. 1 then becomes the *asymmetric* D1Q3 lattice shown in fig 2, whose velocities are

$$
V_0 = \frac{v}{2}, \qquad V_1 = \frac{3v}{2}, \qquad V_2 = -\frac{v}{2}
\tag{8}
$$

The local equilibrium distributions given in eq. (6) can be transformed by com-

puting them for $u - U$. With $U = v/2$ they become

$$
\begin{aligned}
f_0^{eq} &= \tfrac{3}{4}h - \tfrac{1}{v^2}\left(\tfrac{1}{2}gh^2 + hu^2\right) + \tfrac{1}{v}hu \\
f_1^{eq} &= -\tfrac{1}{8}h + \tfrac{1}{2v^2}\left(\tfrac{1}{2}gh^2 + hu^2\right) \\
f_2^{eq} &= \tfrac{3}{8}h + \tfrac{1}{2v^2}\left(\tfrac{1}{2}gh^2 + hu^2\right) - \tfrac{1}{v}hu
\end{aligned}
\tag{9}
$$

It is easy to check that, with the above local equilibrium distributions, we still obtain the expected moments for a SW model, namely

$$
\sum_i f_i^{eq} = h, \qquad \sum_i f_i^{eq} V_i = hu,
\tag{10}
$$

and

$$
\sum_i V_i^2 f_i^{eq} = \frac{1}{2}gh^2 + hu^2
\tag{11}
$$

This is a general consequence of the fact that $V_i = v_i + U$ and $f_i^{eq}(h, u) = \hat{f}_i^{eq}(h, u - U)$, where $\hat{f}_i^{eq}$ is the local equilibrium distribution of the standard LB model. Indeed, we have $\sum_i f_i^{eq}(h, u) = \sum_i \hat{f}_i^{eq}(h, u - U) = h$ and

$$
\begin{aligned}
\sum_i V_i f_i^{eq}(h, u) &= \sum_i (v_i + U)\hat{f}_i^{eq}(h, u - U) \\
&= \sum_i v_i \hat{f}_i^{eq}(h, u - U) + U \sum_i \hat{f}_i^{eq}(h, u - U) \\
&= h(u - U) + Uh = hu
\end{aligned}
\tag{12}
$$

and finally

$$
\begin{aligned}
\sum_i V_i^2 f_i^{eq}(h, u) &= \sum_i (v_i + U)^2 \hat{f}_i^{eq}(h, u - U) \\
&= \sum_i v_i^2 \hat{f}_i^{eq}(h, u - U) + 2U \sum_i v_i \hat{f}_i^{eq}(h, u - U) \\
&\quad + U^2 \sum_i \hat{f}_i^{eq}(h, u - U) \\
&= \frac{1}{2}gh^2 + h(u - U)^2 + 2Uh(u - U) + U^2 h \\
&= \frac{1}{2}gh^2 + hu^2
\end{aligned}
\tag{13}
$$

In 1D systems, the three equilibrium populations are entirely defined by the

5

expressions of the above first three moments. We could have used such an approach to derived f^{eq} for the asymmetrical model, instead of the Galilean transformation. However, in 2D, there are not enough moments to computed uniquely the equilibrium populations, but the Galilean transformation could still be used.

With our choice of V_i's the streaming part of the LB dynamics moves the distributions f_i to half-integer and integer sites of the lattice. To avoid this problem we can rescale the velocities by a factor of 2. This is equivalent to change v in $2v$ in eq. (9). Thus, with

$$V_0 = v, \qquad V_1 = 3v, \qquad V_2 = -v \tag{14}$$

the local equilibrium functions are

$$\begin{array}{rcl}
f_0^{eq} & = & \frac{3}{4}h - \frac{1}{4v^2}\left(\frac{1}{2}gh^2 + hu^2\right) + \frac{1}{2v}hu \\
f_1^{eq} & = & -\frac{1}{8}h + \frac{1}{8v^2}\left(\frac{1}{2}gh^2 + hu^2\right) \\
f_2^{eq} & = & \frac{3}{8}h + \frac{1}{8v^2}\left(\frac{1}{2}gh^2 + hu^2\right) - \frac{1}{2v}hu
\end{array} \tag{15}$$

These expressions, together with eq. (5) and

$$h = \sum_i f_i, \quad hu = \sum_i V_i f_i \tag{16}$$

define the asymmetric LB model for 1D shallow water flows.

3.2. Chapman-Enskog expansion

A multiscale Chapman-Enskog expansion can be considered in order to confirm that the above asymmetric LB model gives the expected SW equations in the continuous limit, and for low dissipation ($\tau \approx 1/2$). For this purpose, we write f_i as $f_i = f_i^{eq} + f_i^{neq}$, we perform a second order Taylor expansion of the LB equation, and we take the first two moments. Following the standard procedure (see for instance [6] where it is done in detail for the 1D LB shallow

6

water model), we obtain

$$\partial_t h + \partial_x (hu) = 0 \tag{17}$$

$$\partial_t (hu) + \partial_x \left(\Pi^{eq} - \Gamma \right) = 0 \tag{18}$$

where Γ, the dissipative current is

$$\Gamma = \Delta t \left(\tau - \frac{1}{2} \right) \left[-\frac{\partial \Pi^{eq}}{\partial h} \partial_x hu - \frac{\partial \Pi^{eq}}{\partial hu} \partial_x \Pi^{eq} + \partial_x S^{eq} \right] \tag{19}$$

and the quantities Π^{eq} and S^{eq} are defined as

$$\Pi^{eq} = \sum_i V_i^2 f_i^{eq} \qquad S^{eq} = \sum_i V_i^3 f_i^{eq} \tag{20}$$

The above equations are very general and requires only the definition (16) of h and u, and the conservation laws imposed by (10). Therefore they are structurally identical to those obtained when analyzing the standard 1D LB SW model. Since our equilibrium distributions (15) lead to the same second moment Π^{eq} as the standard LB model, the only difference of the asymmetrical model is due to the new expression of S^{eq} in the right hand side of the dissipative term eq. (19).

A straightforward calculation gives

$$S^{eq} = v^2 hu + 3v \left(\frac{1}{2} g h^2 + hu^2 \right) - 3hv^3 \tag{21}$$

The last two terms of this equation are not present in the symmetric LB SW equation. This modification only affects Γ, the dissipative part of eq. (18) which is found to be

$$\Gamma = \Delta t \left(\tau - \frac{1}{2} \right) \left[\left(-gh - 3u^2 + 6uv + v^2 \right) \partial_x hu + \left(-2ghu + 3ghv + 2u^3 - 3v^3 - 3u^2 v \right) \partial_x h \right] \tag{22}$$

in the present asymmetric D1Q3 model. This has to be compared with the

7

expression found in the standard D1Q3 symmetric model [6]

$$\Gamma = \Delta t \left(\tau - \frac{1}{2}\right) \left[\left(-gh - 3u^2 + v^2\right)\partial_x hu + \left(-2ghu + 2u^3\right)\partial_x h\right] \qquad (23)$$

In the usual SW equation (1), Γ is neglected. And if not, there is no commonly accepted form of the dissipation term in the literature. We showed in [6] that the 1D LB SW equation can be considered for values very close to $\tau = 1/2$, without numerical instabilities. Therefore, in this limit, our asymmetric LB model correctly reproduces the standard SW equation.

3.3. Stability analysis

In this section, we consider a stability analysis of the asymmetrical SW LB model and show that no more restriction on the value of the Froude number are expected. We first discuss linear stability by considering a small deviation from a steady solution. This approach has been used previously by many authors. See for instance [8, 9]. For the shallow water, a full derivation is given in [6], for the symmetric 1D LB model.

We consider a small perturbation ϵ_i around a steady solution $f_i = f_i^{eq}(h_0, u_0)$. In terms of the perturbation ϵ_i, the LB shallow water equation becomes

$$\begin{pmatrix} \epsilon_0(x, t + v\Delta t) \\ \epsilon_1(x + 3v\Delta t, t + \Delta t) \\ \epsilon_2(x - v\Delta t, t + \Delta t) \end{pmatrix} = M \begin{pmatrix} \epsilon_0(x, t) \\ \epsilon_1(x, t) \\ \epsilon_2(x, t) \end{pmatrix} \qquad (24)$$

where M can be computed from the expression of f^{eq} of the asymmetrical model. The stability of the numerical model depends on the eigenvalues λ of M. They can be obtained analytically in the Fourier space. The calculation is rather tedious and won't be given explicitly here as it follows the same steps as described in [6]. Out of the three eigenvalues, two of them, $\lambda_\pm$ have value 1 when the wave number k goes to zero. They correspond to the conserved modes, h and hu. The third eigenvalue corresponds to a ghost mode and has

8

a value smaller than one for $k \to 0$. It will thus not affect that stability of the hydrodynamic regime. The result is

$$\lambda_\pm = e^{i\beta_\pm k} e^{-\eta_\pm k^2 (\Delta x)^2}$$

where

$$\beta_\pm = \frac{\pm 1 - \text{Fr}}{\Psi} \qquad (25)$$

and

$$\eta_\pm = \mp \frac{1}{2} \left(\tau - \frac{1}{2} \right) (\text{Fr} \pm + \Psi) (\text{Fr} \pm -3\Psi) (\text{Fr} \pm -\Psi) / \Psi^2 \qquad (26)$$

where $\Psi = v/\sqrt{gh_0}$ is defined as the lattice Froude number.

The numerical scheme become unstable when $\eta_\pm < 0$. This defines the linear stability zone, as shown in light gray in Fig. 3. Compared to the stability region of the standard model (dark gray), we have now no more limits on the value of Fr. This stability region is not affected by the value of τ, as long as $\tau \geq 1/2$.

Note that in the asymmetrical model, the lattice Froude number $\Psi = v/\sqrt{gh}$ can be smaller than 1. It means that surface waves can travel faster than v, the reference lattice speed. This is actually not a contradiction as the maximum lattice speed is $3v$ in this model.

The above results can be confirmed numerically by running simulations that sample the possible values of Fr and Ψ. A periodic 1D flow with uniform speed u and uniform water level h is considered, with a small Gaussian perturbation of the water height. In these simulations, the non-linearity of the dynamics is preserved.

It is observed, in accordance with the analytical study, that the stability region is entirely defined by

$$\Psi + 1 < \text{Fr} < 3\Psi - 1 \qquad \Psi - 1 < Fr < \min(\Psi + 1, 3\Psi - 1) \qquad (27)$$

Expressed in terms of the velocity variables, these relations take the form of

9

Courant-like conditions

$$\text{Fr} < 1 : \qquad -v < u - \sqrt{gh} \text{ and } v < u + \sqrt{gh} < 3v$$

$$\text{Fr} > 1 : \qquad u - \sqrt{gh} < v < u + \sqrt{gh} < 3v$$

$$(28)$$

Therefore our asymmetric LB model is stable at the fluvial-torrential transition.

4. Numerical validations

4.1. Flow with Fr > 1

In this section we investigate whether our asymmetric LB model properly computes the water profile in the case of a flow with Fr > 1. We consider a simulation of the flow in a canal in which both the water height and the water speed is imposed at the inlet. The Froude number at the inlet is Fr = 2.35. At the outlet, a zero gradient condition is set on f_2. In addition, we also include in the LB model an external force F which mimics the slope of the canal and some friction at the bottom.

Note that different ways exist to add the external force on the LB scheme (see [10, 4, 6] for examples). These different options have been tested and they affect the accuracy of the solution. The so-called *simple* force scheme is obtained by adding a quantity F_i to eq. (5). To compute F_i as a function of the external force F, mass conservation imposes

$$\sum_i [f_i(x + v_i \Delta t, t + \Delta t) - f_i(x, t)] = F_0 + F_1 + F_2 = 0 \qquad (29)$$

and momentum balance requires

$$\sum_i V_i [f_i(x + v_i \Delta t, t + \Delta t) - f_i(x, t)] = v(F_0 + 3F_1 - F_2) = Fdt \qquad (30)$$

whose solution is

$$F_0 = \frac{F\Delta t}{2v} - 2F_1 \qquad F_2 = -\frac{F\Delta t}{2v} + F_1 \tag{31}$$

Lattice directions 0 and 2 being symmetrical, we choose to also impose $F_0 = -F_2$, from which we get $F_1 = 0$. As a result, the quantities F_i can be written in the usual form as $F_i = w_i \Delta t V_i F/c_s^2$, with $w_0 = 1/2$, $w_1 = 0$, $w_2 = 1/2$, $c_s^2 = v^2$.

The Zhou's force term is added by using the expression proposed in [4]

$$F_i = w_i \frac{\Delta t}{c_s^2} V_i F_i' \tag{32}$$

with

$$F_0' = F\left(x + \frac{\Delta x}{2}\right), \quad F_1' = 0, \quad F_2' = F\left(x - \frac{\Delta x}{2}\right) \tag{33}$$

The Guo-Chopard's force term, defined in [6], is calculated as

$$F_i = w_i \left(1 - \frac{1}{2\tau}\right) \frac{\Delta t}{c_s^2} V_i F \tag{34}$$

but in this case, the definition of u in terms of the f_i's becomes

$$hu = \sum_i v_i f_i + \frac{\Delta t}{2} F \tag{35}$$

The parameters of the simulation are summarized in table 1.

In fig. 4, we compare the water profile along the canal as obtained from our LB simulation with results produced by other numerical solvers, commonly used to solve the time-dependent shallow water equation. These extra solvers are the implicit finite difference Preissmann solver [11] and a finite volume (FV) solver [12, 13]. We can see that the solution provided by our asymmetrical LB model is very good when compared to a reference solution obtained by a high accuracy solution of the time-independent shallow-water equation (1). For the three methods shown in fig. 4, the water discharge hu is constant within less

11

than 0.05%.

We consider several spatial resolutions by changing the number of lattice points N_x representing the canal length. The results are given in fig. 5, once the steady state is reached. We see that our LB model is first order accurate with the lattice spacing Δx when compared to the reference profile. From theoretical grounds, the LB SW is expected to be second order accurate. Boundary conditions are a well known reasons to loose the second order accuracy. Another reason is the fact that the reference solution is without dissipation, whereas the LB model has a residual one. Finally, the external force may also be responsible for a reduce accuracy level.

4.2. Transition from a torrential to a fluvial regime

Our final test is to study the capability of the asymmetric LB SW model to simulate a transition from a flow with Fr > 1 (termed torrential regime) to a flow with Fr < 1 (termed fluvial regime). We consider a simulation similar to that of the previous section but with different values of the setting (see table 2), so as to produce a transition around the middle of the canal. The steady state result of the simulation is shown in fig. 6 for a system of size $N_x = 128$, for the LB, FV and Preismann solvers. Note that, in this experiment, only the *simple* force scheme defined above turned out to be a numerically stable way of adding the external force F in the asymmetric LB scheme.

We observe that all solvers agree well except close to the transition region, where quantitative differences show up. In the LB simulations the jump in water height is less sharp than that computed by the other methods. However, by increasing N_x, we can reduce the width of the transition region at will.

For both the Preismann and LB scheme, we observe a slight decrease of the water current hu after the transition. For the LB case, this is due to the fact that the *simple-force* approach can cause a small deviation to the continuity

12

equation when F is not constant in space or time.

The Rankine-Hugoniot [14] conditions for the stationary case require that the quantity

$$M(h) = \frac{q^2}{gh} + \frac{h^2}{2} \tag{36}$$

must be preserved before and after the shock, where $q = hu$ is the discharge. This can be explained by observing that $M(h)$ is simply the flux of momentum $gh^2/2 + hu^2$ that appears in eq. (1) divided by the gravity constant g. Let us denote by x_1 and x_2 the locations just before and just after the transition. By integrating the momentum equation $\partial_t hu + \partial_x gM = F$ across the jump, we have, in a steady state $(\partial_t hu = 0)$,

$$\int_{x_1}^{x_2} \partial_x M(h(x)) \; dx = \frac{1}{g} \int_{x_1}^{x_2} F(x) \; dx \tag{37}$$

If we assume that the transition is sharp $(x_2 \approx x_1)$, we are left with $M(h_2) - M(h_1) = 0$, where $h_1 = h(x_1)$ and $h_2 = h(x_2)$.

The value of M versus h is shown in Fig. 7 for the three numerical methods. The points M in the plot correspond to the values of $h^2/2 + q^2/(gh)$, with h and $q = hu$ measured from the simulation along the x-axis.

We can see that $M(h_1) = M(h_2)$ to a good accuracy in all three cases (less that 10^{-4}). For the LB case, we also observe that $M(h)$ is not constant across the jump: it starts decreasing until the middle of the transition and then increases again so that, finally $M(h_1) \approx M(h_2)$.

To explain these observations, we should take into account the finite width of the water jump and the dissipative term Γ for the LB solver. For any x in the transition region, we obtain,

$$\int_{x_1}^{x} \partial_x \left[M(h(x)) - \frac{\Gamma}{g} \right] \; dx = \frac{1}{g} \int_{x_1}^{x} F(x) \; dx \tag{38}$$

13

and thus

$$M(h(x)) - M(h_1) = \frac{1}{g} \left(\Gamma(x) - \Gamma(x_1) \right) + \frac{1}{g} \int_{x_1}^{x} F(x) \ dx \qquad (39)$$

If we choose $x = x_2$ we have $\Gamma(x_1) \approx \Gamma(x_2) \approx 0$ because the water profile at x_1 and x_2 is almost flat and, as seen from (22) we can neglect the dissipation. Therefore we have $M(h_2) - M(h_1) \approx \epsilon$, where ϵ is defined as $\epsilon = \int_{x_1}^{x_2} F(x)/g \ dx$. We can approximate the integral of F as $(\partial x/\partial h) \int_{h_1}^{h_2} (F(h)/g) \ dh$ because h varies almost linearly across the jump. With $F(h) = gh(I - J)$ where J is given by (2) and $u = q/h$, we obtain, with a numerical integration, $\epsilon = -5.3 \times 10^{-5}$.

This is compatible with the departure from the Rankine-Hugoniot relation observed in the three numerical simulations. For instance, for the LB case, we have $h_1 = 0.065$, $h_2 = 0.094$, $M(h_1) = 0.00978$, $M(h_2) = 0.00972$, and thus $M(h_2) - M(h_1) = -6 \times 10^{-5}$

We can also explain why, with the LB simulations, the value of M goes from $M(h_1)$ to $M(h_2)$ as a smooth curve. This is due to the dissipation Γ, which is non-zero across the water jump. For the two other solvers, there is no viscous term and the transition of M is more abrupt. This can be quantified by using eq. (39) for $x = x_m = (x_1 + x_2)/2$. By neglecting the integral over F in comparison to $\Gamma(x_m)$ and with again $\Gamma(x_1) \approx 0$ one has $M(h(x_m)) - M(h_1) = \Gamma(x_m)/g = -0.00024$. This is compatible with the distance observed on Fig. 7 between the minimum of M and $M(h_1)$.

Finally, we can also compare the ratio h_2/h_1 observed in the simulation with Bélanger's equation [1]

$$\frac{h_2}{h_1} = \frac{1}{2} \left(\sqrt{1 + 8\mathrm{Fr}_1^2} - 1 \right) \qquad (40)$$

which predicts the water heights h_1 and h_2 before and after the water jump, where Fr_1 is the Froude number in the torrential regime. This equation gives the

ratio between the two solutions h_1 and h_2 of $M(h) = $ const, for $q = h_1 u_1 = h_2 u_2$.

With the LB simulations, one has $h_1 = h(x = 3.8) = 0.065$, $h_2 = h(x = 4.8) = 0.094$ and $Fr_1 = 1.32$. According to eq. (40) the value of h_2 should be

$$h_2 = \frac{h_1}{2} \left(\sqrt{1 + 8Fr_1^2} - 1 \right) = 0.093 \tag{41}$$

in good agreement with the numerical result.

Our asymmetric LB model can also be tested against the experimental data obtained by Gharangik and described in [15] (in the horizontal case). The result of the comparison is shown in Fig. 8. The simulation (solid line) reproduces very well the jump of the water height observed experimentally (squares). The situation corresponds to a rectangular straight channel of length $L = 13.9$ m and width $B = 0.45$ m, with an imposed flow $Q = 0.053$ m^3/s. From the experimental data, the water levels at the beginning and the end of the channel section are $h(0) = 0.064$ m and $h(L) = 0.165$ m, respectively. In the simulation, we used these two values as boundary conditions. Another boundary condition is the inlet velocity, which was set to $u(0) = 1.82$ m/s to have the correct discharge $Q = Bh(0)u(0)$.

In the experiment, the Manning coefficient n was found to range from 0.008 to 0.011 (see [15]). In the simulation, $n = 0.007$ gave the best agreement with the experimental points, that is a jump that starts at $x = 1.5$ m. This location is sensitive to the value of n chosen in the simulation. Increasing n was found to move the jump in the upstream direction. The width Δ of the jump is dependent on the value of the relaxation time τ of the LB model, which is related to the dissipation. With $\tau = 0.85$ we obtain a good agreement with the experimental findings, that is $\Delta = 1.2$ m. By lowering τ, the steepness of the jump is increased, and a little overshoot may be created at the upper part of the jump.

15

5. Conclusions

In this paper, we have proposed a new lattice Boltzmann (LB) model which can describe 1D shallow water flows at Froude numbers larger than 1, a regime which is numerically unstable with the standard lattice Boltzmann shallow water approach. This models allows us to simulated the fluvial-torrential transition, which is known to be a difficult task.

Our new model can be derived by performing a Galilean transformation of the standard one. It results in a asymmetrical velocity lattice, well appropriate to describe a flow with large velocity in one direction.

Galilean transformations have already been used in the LB literature as a way to design numerical models. For instance, in [16, 17] the collision rule of a LB fluid is built on the Galilean invariant (central) moments of the density distribution functions f_i. In [18], a Galilean transformation is applied to the f_i's in order to derive a Lees-Edwards boundary condition for a fluid subject to an imposed shear rate. In that same paper, a Galilean transformation is also used to compute the change of f_i due to the interaction between the fluid and a moving suspension. However, in all these cases, the Galilean transformation is only applied to the f_i or their moments. In our asymmetric model, the transformation also affects the lattice velocities v_i.

It should be noted that with the coupling methods described in [6, 7] we can expect to couple our asymmetrical D1Q3 model with a symmetric one and then to describe a canal system with sections having quite different flow regimes.

It was shown in [6] that the standard 1D LB SW is computationally more effective than the Preismann or FV solvers, for the same, or even higher, level of accuracy. The weakness of the standard 1D LB SW model is its stability range. With the asymmetrical LB model, we have corrected this problem, by moving and shaping the numerical stability domain in order to cope with all

16

Froude numbers.

A 2D generalization of the asymmetrical SW-LB is possible but numerical simulations should still be performed in order to check its stability and accuracy. In a future study, we also plan to test our approach in the context of general LB models.

We thanks Guy Simpson for providing us with the Finite Volume solver of the shallow water equation used in our comparisons and Santosh Ansumali for interesting comments on our approach.

References

[1] W.H. Graf and M.S. Altinakar. *Hydraulique fluviale - Ecoulement et phénomènes de transport dans les canaux â géométrie simple*, volume 16 of *Traité de génie civil de l'Ecole Polytechnique Fédérale de Lausanne*. Presses Polytechniques Universitaires Romandes, 2000. ISBN 978-2-88074-812-8.

[2] R. Salmon. The lattice Boltzmann method as a basis for ocean circulation modeling. *J. Marine Resarch*, 57:503–535, 1999.

[3] P.J. Dellar. Nonhydrodynamic modes and a priori construction of shallow water lattice boltzmann equation. *Phys. Rev. E*, 65:036309, 2002.

[4] J.G. Zhou. *Lattice Boltzmann Methods for Shallow Water Flows.* Springer, 2004.

[5] J.B. Frandsen. A simple lbe run-up model. *Progress in Computational Fluid Dynamics*, 8:222–232, 2008.

[6] Pham van Thang, Bastien Chopard, Laurent Lefèvre, Diemer Anda Ondo, and Eduardo Mendes. Study of the 1d lattice Boltzmann shallow water equation and its coupling to other models. *J. Comp. Physics*, 229:7373–7400, 2010.

[7] Pham van Thang. Modélisation et commande des systèmes non-linéaire à paramètres distribués par la méthode de Boltzmann sur réseau: application aux canaux d'irrigation. Technical report, Grenoble INP ESISAR, France, 2009. Master disertation.

[8] J.D. Sterling and S. Chen. Stability analysis of lattice boltzmann methods. *J. Comp. Phys*, 123:196–206, 1996.

[9] P. Lallemand and L.S. Luo. Theory of the lattice boltzmann method: Dispersion, dissipation, isotropy, gallilean invariance, and stability. *Phys. Rev. E*, 61(6):6546, 2000.

[10] Zhaoli Guo, Chguang Zheng, and Baochang Shi. Discrete lattice effects on forcing terms in the lattice Boltzmann method. *Phys. Rev. E*, 65:046308, 2002.

[11] Jean-Francois DULHOSTE. *Contribution à la commande non linéaire de systèmes d'irrigation*. PhD thesis, Laboratoire d'Automatique de Grenoble, novembre 2001.

[12] Guy Simpson and Sébastien Castelltort. Coupled model of surface water flow, sediment transport and morphological evolution. *Computers & Geosciences*, 32:1600–1614, 2006.

[13] E.F. Toro. A weighted average flux method for hyperbolic conservation laws. *Proc. R. Soc. Lond.*, pages 401–418, 1989.

[14] D. Serre. *Hyperbolicity, Entropies, Shock Waves*. Cambridge University Press, 1999.

[15] Thomas Molls and M. Hanif Chaudhry. Depth-averaged open channel flow model. *J. Hydr. Eng. Div. ASCE*, 121:453–465, 1995.

[16] M. Geier, A. Greiner, and J.G korvink. Cascadaded digital lattice Boltzmann automata for high Reynolds number flow. *Phys. Rev. E*, 73:066705, 2006.

[17] M. Geier, A. Greiner, and J.G Korvink. A factorized central moment lattice Boltzmann method. *Eur. Phys. J. Special Topics*, 171:55–61, 2009.

[18] Alexander J. Wagner and Ignacio Pagonabarraga. Lees-Edwards boundary conditions for Lattice Boltzmann. *J. Stat. Phys.*, 107(1/2):521–537, 2002.
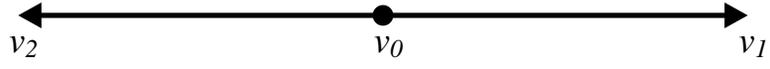
Figure 1: Lattice Boltzmann D1Q3 velocities $v_0 = 0$, $v_1 = v$ and $v_2 = -v$, with $v = \Delta x/dt$.
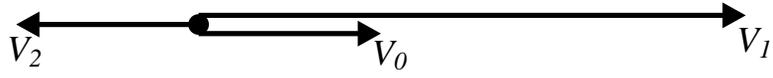
Figure 2: The asymmetric D1Q3 lattice obtained from a Galilean transform with speed 1/2.
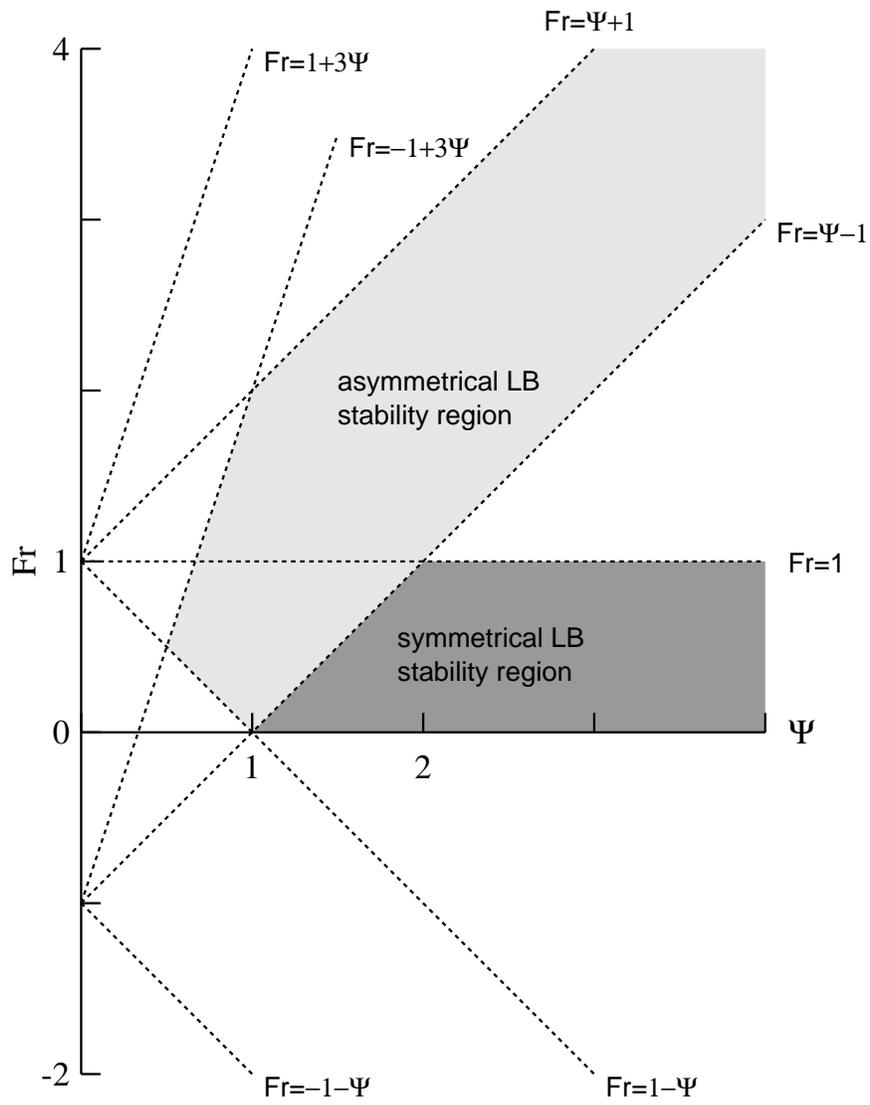
Figure 3: The stability region of the symmetrical and asymmetrical LB models, in terms of the two dimensionless numbers, the Froude number Fr and the lattice Froude number Ψ.
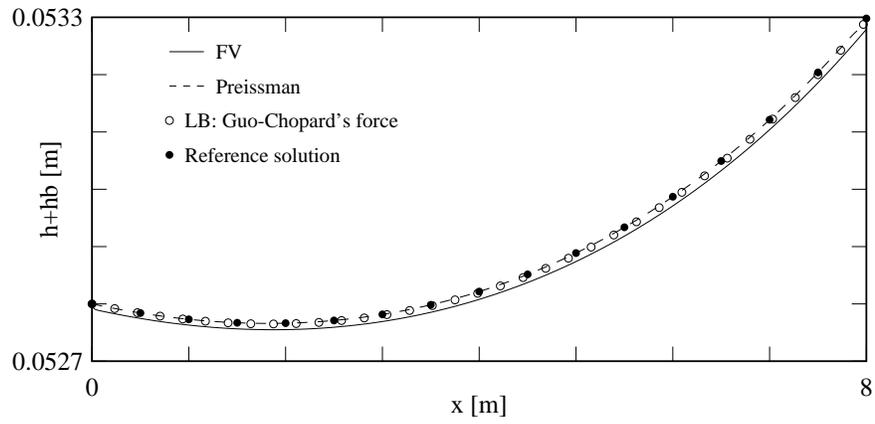
Figure 4: Validation of the asymmetric LB model to describe the solution of the shallow water equation with Froude number larger than 1, and $N_x = 512.$. The water profile is compared with two well tested numerical solvers in a steady state regime, and a high precision numerical solution of the steady SW eq. (1), coined "reference" solution in the figure.
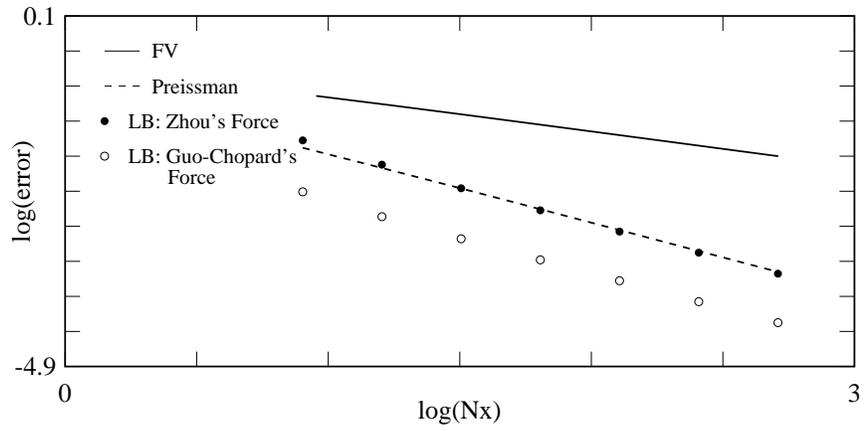
Figure 5: Accuracy plot of the convergence of the numerical solutions to the reference profile, for the plots in fig. 4. The error as a function of the spatial resolution is shown. Different ways to add the external force are considered for the LB scheme. See [6] for a definition of the types of forces.
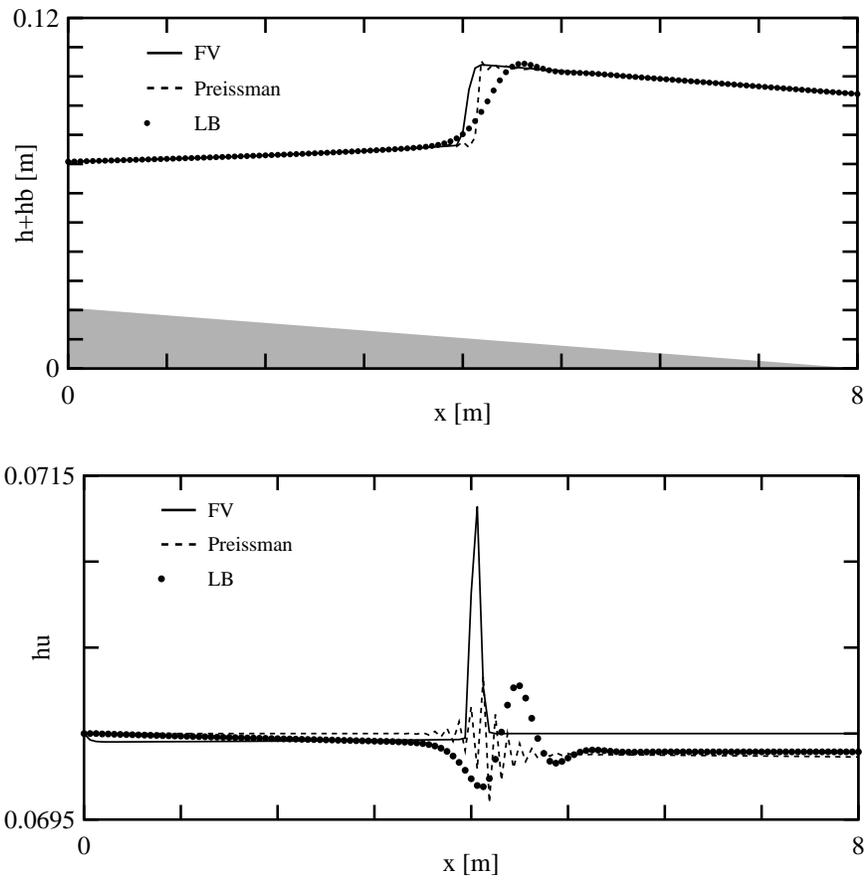
Figure 6: Water profile (upper panel) and discharge (lower panel) in a torrential-fluvial transition, for different numerical solvers. The shaded area represents the bed profile. The spatial discretization is $N_x = 128$. For the LB simulation, the relaxation time is $\tau = 0.6$.
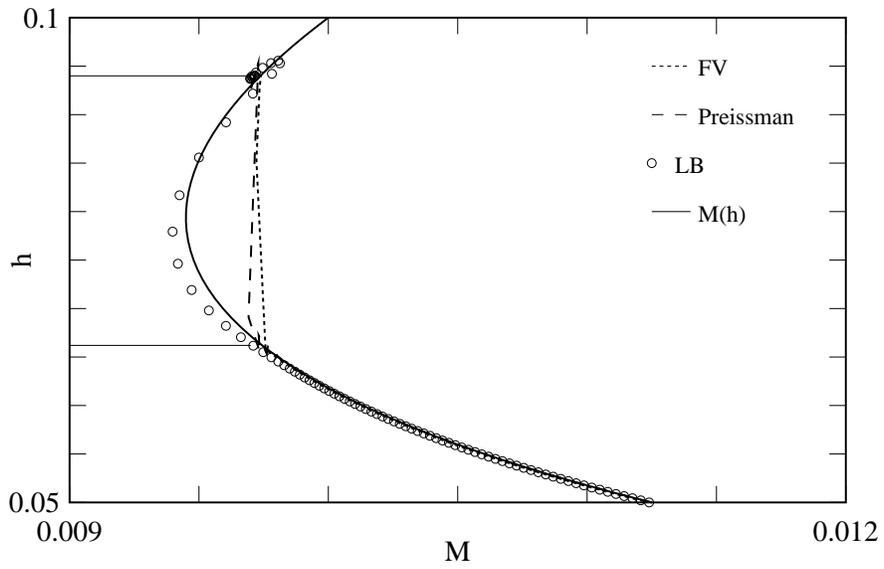
Figure 7: Test of the Rankine-Hugoniot relation across the transition, with $q = 0.07$. The two horizontal segments indicate the observed water heights before and after the shock. Their values are $h_1 = 0.065$ and $h_2 = 0.094$.
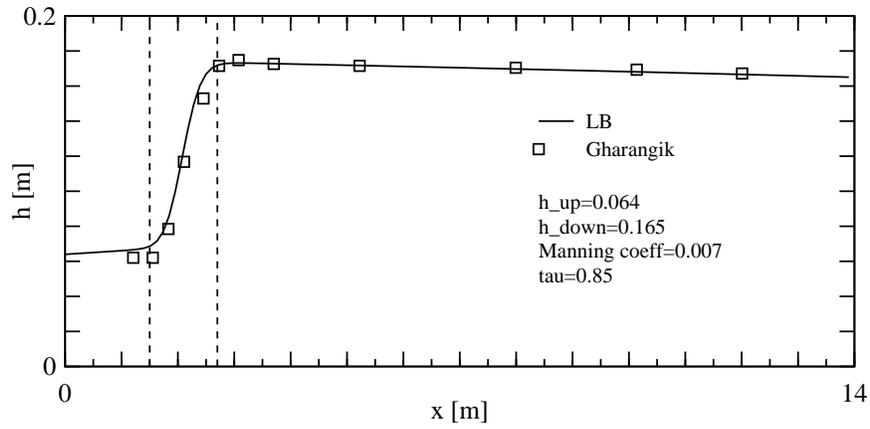
Figure 8: Water height in the case of the hydraulic jump experiment by Gharangik [15]. Measurements (squares) are compared to a numerical simulation with the asymmetrical LB (solid line). The simulation contains $N_x = 128$ lattice points. The two vertical dashed lines indicate the beginning and end of the jump, as described in [15].

Canal length	L	8 m
Canal width	B	0.1 m
Canal slope	I	1.6e-3
Coefficient of friction	n	0.005
relaxation time	τ	1
Upstream water height	h_{up}	0.04 m
Upstream velocity	u_{up}	1.4725 m/s
lattice speed	v	1.5 m/s

Table 1: Parameters of the simulation with Froude number Fr = 2.35.

Canal slope	I	2.6e-3
Friction coefficient	n	0.007
Upstream water level	h_{up}	0.05 m
Upstream velocity	u_{up}	1.4 m/s
Lattice spacing	Δx	0.0625 m
Lattice speed	v	1.5 m/s

Table 2: Parameters of the simulation showing the torrential-fluvial transition.